Design of unpaved forest roads - stress-strain response of a reinforced soil under triaxial conditions

David Carlos[1], *Olávio* Cafôfo[2], *Joaquim* Macedo[1], and *Margarida* Pinho-Lopes[1*]

[1]CERIS—University of Aveiro, Department of Civil Engineering, 3810-193 Aveiro, Portugal
[2]Megavia – Construções e Obras Públicas, SA, 2400-119 Leiria, Portugal

Abstract. Often, the design and construction of unpaved forest roads makes use of locally available soils. The road cross section consists of a base layer formed by locally available soil, good-quality aggregate or a mixture of these materials. To decrease the quantity of good-quality aggregates required for building such layer, using locally sourced soils is favoured. Including layers of geosynthetic reinforcements will contribute to reducing the quantities of granular material forming the base layer and/or increase its mechanical properties. This paper studied the influence of single pocket geocells on the mechanical response of a locally sourced soil (well-graded sand with gravel) close to an unpaved forest road (Aveiro, Portugal). The geocells were 3D printed, to define a reinforcement geometry adjusted to the soil characteristics, namely in terms of particle size distribution. The mechanical response of the composite material was characterised using triaxial tests. This allowed assessing its stress-strain response and any changes relatively to the unreinforced soil. The strength parameters of the composite material were estimated using equations from the literature. The study demonstrates that the inclusion of single pocket geocells enhanced the mechanical properties of the soil. These geocells increased the soil's peak friction angle and provided additional confining stresses.

1 Introduction

Unpaved forest roads play a crucial role in forest management, providing essential access for activities such as harvesting, transportation, and conservation. These roads are typically constructed using locally available materials, which often include soils of varying quality. While cost-effective, the reliance on such materials can lead to performance issues, particularly under repeated loading and challenging environmental conditions. Addressing these limitations through sustainable and innovative solutions is vital for ensuring the durability and functionality of forest road networks.

Sustainable construction and maintenance of unpaved roads has gained increasing attention in recent years. Reducing the environmental footprint of these infrastructures requires minimizing the use of high-quality aggregates and incorporating locally sourced

* Corresponding author: mlopes@ua.pt

materials wherever possible. Reinforcing these materials offers an opportunity to achieve this goal, while improving the mechanical properties of the unpaved roads layers.

Geosynthetic reinforcements, such as geocells, have emerged as effective solutions for enhancing the performance of unpaved roads. Geocells confine soil particles, increase load-bearing capacity, and reduce deformation under stress. While traditionally manufactured, geocells have shown promising results [1-3]. Recent advances in product development processes, in particular 3D printing, enable the development of customized reinforcement geometries tailored to specific soil characteristics [e.g., 4-6]. This approach offers a pathway to explore new designs and optimize reinforcement performance.

This is an exploratory study that aims to investigate the stress-strain response of a locally sourced soil reinforced with 3D printed single pocket geocells, via triaxial tests. The objectives include evaluating the mechanical performance of the reinforced soil, comparing the effects of different geocell geometries, and analysing their potential to reduce reliance on high-quality aggregates. To achieve these objectives, an experimental program was conducted, including the characterization of soil properties, the design and fabrication of geocells using 3D printing, and triaxial testing of unreinforced and reinforced soil specimens.

2 Materials and methods

2.1 Experimental programme

The experimental programme implemented in this study includes the characterization of some relevant properties of the materials: soil; reinforcement; and composite material formed by the soil with the reinforcement (3D printed geocells). Particular attention was given to the stress-strain behaviour of the unreinforced and reinforced soil, assessed using triaxial tests, to analyse and compare the influence of the inclusion of two different geocells.

2.2 Materials

2.2.1 Soil

The soil studied was collected from an unpaved road located in the region of Sever do Vouga, Aveiro (Portugal) (Fig. 1). According to the Unified Soil Classification System (ASTM D2487-11 [7]), the soil is SW-SM, well-graded sand with silt and gravel and is formed by ≈39% of gravel, ≈52% of sand, and ≈9% of fine particles (< 0.075 mm). The particle size distribution was assessed according to EN ISO 933-1: 2012 [8], Fig. 1. Its average particle size (D_{50}) is 2.80 mm and the 10%, 30%, and 60% effective particle size diameters (D_{10}, D_{30}, and D_{60}) are, respectively, 0.11, 0.81 and 4.20 mm. The curvature coefficient (C_C) is 1 and the uniformity coefficient (C_U) is 38. The fine fraction of the soil exhibits non-plastic behaviour, as its plastic limit (w_P) is not quantifiable; its liquid limit (w_L) is 31.0% (tests carried out as described in ISO/TS 17892-12: 2004 [9]). The maximum dry density (γ_{dmax}) and optimum water content (w_{opt}) obtained from modified Proctor tests (ASTM D1557-07 [10] method C), are 19.15 $kN.m^{-3}$ and 4.5%, respectively. The soil particle density (ρ_s), quantified following the pycnometer method (ISO/TS 17892-3: 2004 [11]), is 2.676 $g.cm^{-3}$.

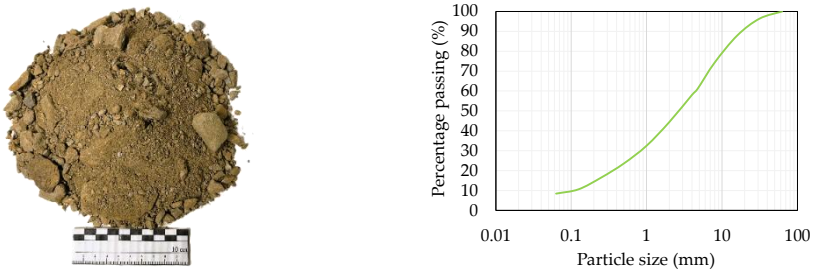

a) b)

Fig. 1. Soil used in the study: a) a sample of soil; b) grain size distribution.

2.2.2 Reinforcement

The reinforcements used to improve the behaviour of the soil were 3D printed geocells, each formed by a single pocket with circular shape (Fig. 2). The main goal for the use of single pocket geocells was to evaluate the influence of their main geometrical aspects. The geocells were designed to optimise their dimensions relative to the infill soil analysed.

The two geocells prototyped (designated as GC075 and GC150) had different dimensions: height (h); diameter (d); and thickness (t). The geometry of both geocells was defined using aspect ratios from the literature and considering the dimensions of the triaxial test specimens tested (diameter, D = 150 mm; height, H = 300 mm) and the grain size distribution of the soil. The two geocells had the same height to diameter ratio, h/d =0.36, and thickness to diameter ratio, t/d = 0.005. The ratios adopted are similar to those reported by Lei *et al.* [5] and in the range of values used in other studies (e.g., [1, 2, 4]).

The diameter of the geocell pocket was defined considering the infill soil studied, represented by the ratios of the maximum particle size (D_{max}) and the average particle diameter (D_{50}) to the geocell pocket diameter (d): D_{max}/d and D_{50}/d. Note that for carrying out triaxial tests, D_{max} must be less than D/6, i.e., 25 mm for the soil studied herein; thus, larger soil particles were removed from the soil specimens. To define the geocells dimensions, corrected values of the maximum particle size and average particle diameter ($D_{max,c}$ and $D_{50,c}$, respectively) were used, referring to the soil tested (after removing particles larger than 25 mm). To study the influence of these ratios on the behaviour of the reinforced soil, they differed for both geocells: $D_{max,c}/d = 0.34$ and $D_{50,c}/d = 0.03$, for GC075; $D_{max,c}/d = 0.17$ and $D_{50,c}/d = 0.02$, for GC150. The values of these ratios for the original soil, would be larger than these, as D_{max} and D_{50} were higher than $D_{max,c}$ and $D_{50,c}$. The values of D_{max}/d and D_{50}/d reported in the literature usually refer to uniform sand [1,2]; herein, as the soil analysed (after the correction mentioned) had a wide particle si0ze distribution (C_U=44), the values for D_{max}/d and D_{50}/d adopted are ~10 times larger.

These design aspects led to two different reinforcement solutions (Fig. 2), placed at mid-height of the triaxial specimens. Geocell GC075 was customised to provide confinement only to the core of the specimen's cross-section, with: h = 27 mm; d = 74 mm; t = 0.4 mm. Geocell GC150 was designed to provide confinement to the entire cross-section of the triaxial test specimen (d ≈ D), with h = 54 mm; d = 148 mm; and t = 0.8 mm (double of those for GC075).

The two geocells prototyped were manufactured using 3D printing with thin fused filament fabrication and the equipment *Creality Ender-3 V3 KE* (Fig. 2a). Thermoplastic Polyurethane, TPU, was the selected polymer as the desired elastic behaviour of commercially available geocells can be replicated. The properties of the TPU filament used are: specific density 1.13 $g.cm^{-3}$; melting temperature 160 °C, tear strength 115 $kN.m^{-1}$; tensile strength at break 28.0 MPa; and elongation at break 700%. Thin fused filament fabrication includes three essential steps: 1) draw the desired digital 3D model, 2) convert

the geometry model into printing instructions (known as slice), and finally 3) print the model. Computer-Aided Design (CAD) software was used to create the digital 3D models for the geocells designed. The slice was done using a free-software, *UltiMaker Cura* version 5.5.0. All geocells were printed using the same nozzle diameter (0.4 mm), bed and nozzle temperature (respectively, 70ºC and 230ºC), layer thickness and height (respectively, 0.4 and 0.2 mm) and printing velocity 30 mm.min^{-1}. To ensure good printing quality, before each printing job, the printer bed was levelled automatically.

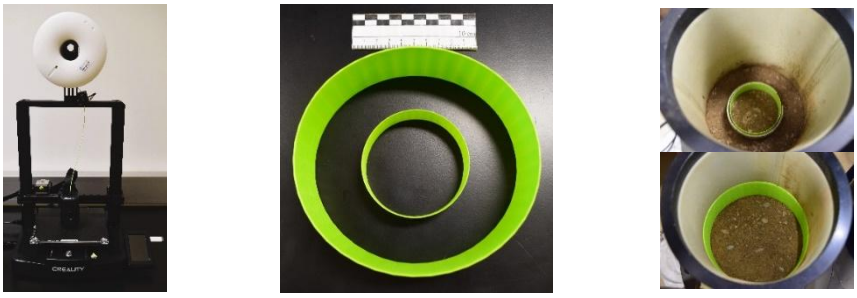

a) b) c)

Fig. 2. Prototyping of geocells: a) 3D printer; b) 3D printed geocells GC075 and GC150; c) geocells inside the triaxial specimens.

2.3 Triaxial tests

Herein, the stress-strain behaviour of the soil, both unreinforced and reinforced, was assessed using triaxial tests. Fully saturated specimens were subjected to consolidated-drained (CD) compression triaxial tests according to the procedure described in ISO/TS 17892-9: 2004 [12]. Cylindrical specimens (Fig. 3; 150 mm diameter and 300 mm height) were subjected to confining stresses of 12, 25 and 50 kPa and sheared at an axial strain rate of 0.2 mm.min^{-1}. Due to equipment constraints, the specimens reached a maximum axial strain of 15%. For this reason, the critical state of the specimens was not reached.

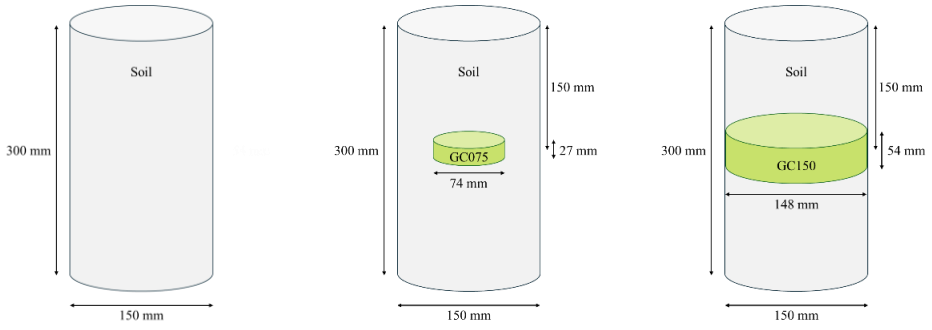

a) b) c)

Fig. 3. Triaxial test specimens: a) unreinforced; b) reinforced with geocell GC075; c) reinforced with geocell GC150.

Each specimen was prepared with 5 layers (60 mm height each) of soil compacted manually, by vibrating the soil and applying cyclic normal forces to each layer. All specimens (unreinforced and reinforced) were prepared with soil compacted to a dry unit weight of 17.24 kN.m^{-3} (corresponding to 90% of $\gamma_{d,max}$ obtained in the modified Proctor test). The

reinforced soil specimens included the geocell reinforcement placed in the central layer (as shown in Fig. 3). The mass of soil used to prepare the reinforced soil specimens was adjusted; the volume of the soil occupied by the geocell was removed.

The particles of soil with sizes larger than 25 mm were removed from the specimens used in the triaxial tests. This is because ISO/TS 17892-12: 2004 [12] mentioned that for nonuniform materials the largest particle size may be up to D/6, i.e., 25 mm for this soil.

2.4 Prediction of equivalent cohesion due to geocell

The effect of including geocells in the soil has been explored by Bathurst and Karpurapu [2], who reference the earlier work of Henkel and Gilbert [13]. This earlier research is frequently employed to estimate the additional confining pressure resulting from membrane action in standard triaxial tests. Fig. 4 illustrates a model that associates the Mohr-Coulomb failure envelope of a soil reinforced with a geocell to that of the corresponding unreinforced soil. In Fig. 4 the enhanced strength of the soil due to geocell confinement is represented in two different ways: i) assuming a homogeneous composite material and, thus, as an equivalent cohesion (c_R), equation 1; ii) as a soil, with the shear strength of the unreinforced soil, and representing the effect of the geocell as an additional confining pressure ($\Delta\sigma_3$). The model assumes that the strength envelopes of both, soil and reinforced soil, are parallel (i.e., $\phi = \phi_R$) and the translation on the y-axis is equal to c_R. The parameters mentioned are: major principal stress (σ_1), minor principal stress (σ_3), major principal stress for the specimens of soil reinforced (σ_{1R}), increased confining stress ($\Delta\sigma_3$), and friction angle for the soil (ϕ) (all parameter is in effective stresses).

The peak friction angle (ϕ_p) was calculated from the results using a linear failure envelope (zero intercept) obtained using the two-dimensional stress invariants, i.e., plotted on a s'-t space. Critical state was not reached, for both unreinforced and reinforced specimens.

$$c_R = \frac{\Delta\sigma_3}{2}\tan\left(\frac{\pi}{4}+\frac{\emptyset}{2}\right) \quad (1)$$

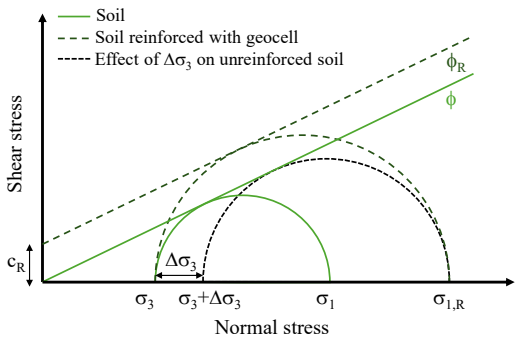

Fig. 4. Model to calculate equivalent cohesion for soil-geocell composites using the Mohr circles (adapted from: Bathurst and Karpurapu [2])

3 Results and discussion

Herein the results are presented and discussed. First, the specimens stress-strain behaviour is presented. The discussion highlights differences in performance between soil and reinforced soil specimens, as well as changes in their failure modes. Strength parameters derived from the test results are then presented. Differences between the peak friction angle of both

unreinforced and reinforced soil specimens are examined, alongside an evaluation of the equivalent cohesion (c_R) and the increase in confining stress ($\Delta\sigma_3$) representing the reinforcement effect. The discussion includes theoretical and practical explanations for the evolution of the behaviour of the materials and the different parameters analysed. Finally, the effect of the aspect ratios considered for modelling the two geocells is discussed.

The data acquired during the triaxial compression tests allows several parameters to be related (such as, stresses, strains, mobilized friction angle, specific volume). The most common way of representing the results obtained is in plots that include the curves deviatoric stress (q) *versus* axial strain (ε_a) and volumetric strain (ε_{vol}) *versus* axial strain. Fig. 5 shows the curves obtained for the different specimens of soil and soil reinforced with geocells GC075 and GC150. The type of failure observed in the different specimens is illustrated in Fig. 6. The aim is to show the impact of the geocells in the soil, represented by the change in stress-strain behaviour and in the failure mode of the reinforced soil, compared to the soil.

The stress-strain curves obtained for the soil specimens are typical of loose materials; no clear peak occurred. The positive volumetric strains, essentially due to volumetric contraction of the specimens, are also in agreement with the above. This is expectable, since the minimum void ratio of the soil, e = 0.37, is considerably lower than the initial void ratio of the test specimens, e = 0.52. The observed failure also agrees with the above: the specimens failed by bulging (typical of loose soils); no shear failure band was detected (Fig. 6a).

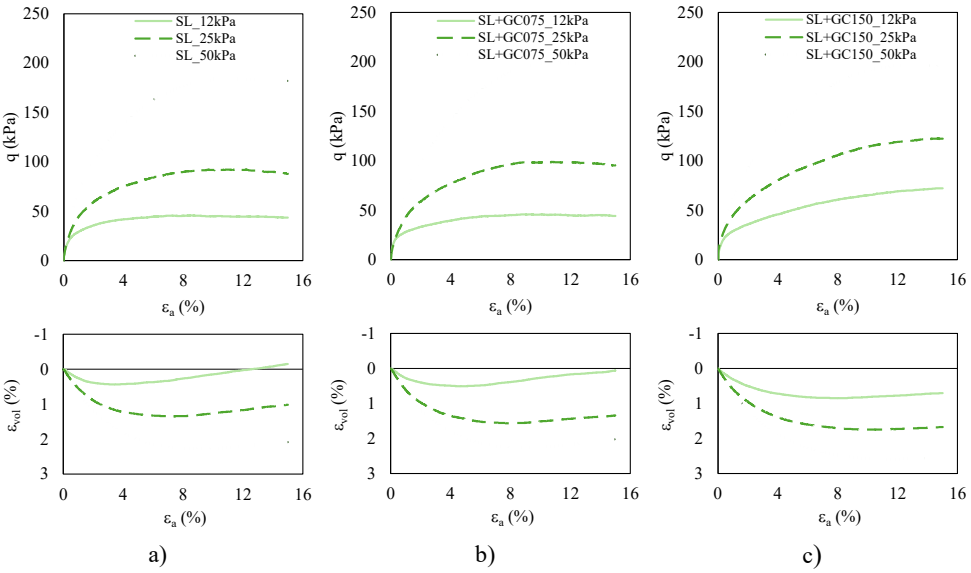

Fig. 5. Stress-strain and volumetric-axial strain behaviour of the test specimens: a) unreinforced; b) reinforced with geocell GC075; c) reinforced with geocell GC150.

The stress-strain behaviour, volumetric deformation and failure mode of the soil were altered by the inclusion of reinforcements, nevertheless in different proportions. Geocell GC075 caused small increments in deviator stress (+0.2% for σ_3=12 kPa; +7.1% for σ_3=25 kPa; +8.2% for σ_3=50 kPa; greater for higher σ_3) and increased the contractile response (more visible in the curve ε_{vol} *versus* ε_a of the specimen tested with σ_3=25 kPa). Such changes may be due to the alteration in the soil's failure mode. These specimens showed a shear failure band below their central zone, where the geocell was placed, i.e., outside the reinforced zone (Fig. 6b). Geocell GC075 provided confinement only to the core of the specimen thus only a small improvement in the soil behaviour was to be expected. In addition, during the assembly of the specimens, the compaction of the soil is made more difficult by geocell, and it is

expected that area of the specimen becomes weaker. This contributed to the change in failure mode and prevented major improvement in the soil behaviour.

The effect of geocell GC150 was better than that of GC075. For GC150, the increments in the deviator stress were greater when lower σ_3 were used (+58.4% for σ_3=12 kPa; +32.8% for σ_3=25 kPa; +6.6% for σ_3=50 kPa); the peak strength of the specimens was reached for larger axial strains; and the contraction of the specimens was more important. Geocell GC150 limited the development of radial strains in the central area of the specimen (Fig. 6c). Because of that, the failure occurred due to bulging of the unconfined portions of the specimen, above and below the geocell. The additional confinement caused by the geocell allowed for an increase in density in the confined zone and, as consequence, enhanced shear strength.

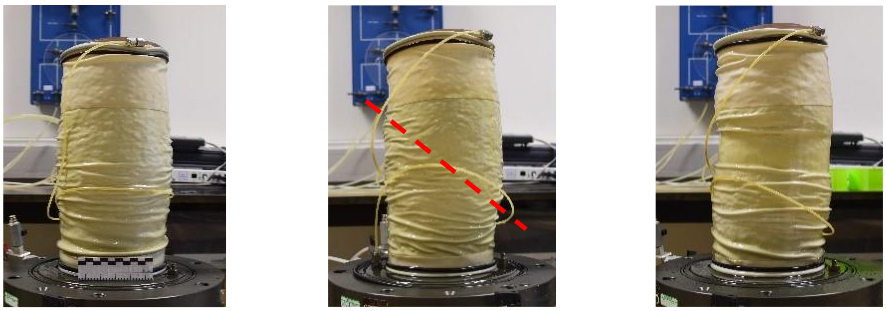

a) b) c)

Fig. 6. Triaxial test specimens' failure modes: a) unreinforced; b) reinforced with geocell GC075; c) reinforced with geocell GC150.

The peak friction angle was calculated as the slope of the Mohr-Coulomb failure envelope represented in an s'-t plot, with zero intercept. The parameters obtained for the soil and the soil reinforced with each of the geocells are compiled in Table 1. The peak friction angle of the soil (40.5º) was in accordance with the ranges of values presented, for example, by Budhu [14] for mixtures of gravel and sand with fine-grained soils (ϕ_p = 30-40º), sands (ϕ_p = 32-50º) and gravels (ϕ_p = 35-50º). The peak friction angles obtained for the soil reinforced with geocells GC075 and GC150 are 41.4º and 43.0º, respectively. Including the geocells increased the peak friction angle of the specimens, more importantly for geocell GC150.

The methodology considered by Bathurst and Karpurapu [2] described in section 2.4 assumes that the friction angle is constant (i.e., $\phi = \phi_R$) and that the effect of the geocells in the soil can be represented as an increase in confining stress or an equivalent cohesion. This methodology was used and resulted in the estimated parameters shown in Table 1. The importance of the increase in confining stress and, consequently, of the equivalent cohesion depended on the geocell and on the confining stress considered in the test. The results showed that the geocells had different effects on the soil. As mentioned, geocell GC075 merely confined a small volume of soil at the core of the tested specimens. As expected, this led to a small increase in confining stress. In addition, the increase in confinement was greater as the test confining stress increased. As mentioned before, the compaction operations for these specimens were affected by the inclusion of the geocell and may have caused a softer and weaker region of the specimen. Before the shear phase, the specimens were saturated and consolidated with volumetric strains (contraction) of the specimens. These deformations increased with higher confining stress applied. This may have reduced the negative effect of the compaction process on the specimens subjected to higher confining stress, improving the stress-strain behaviour and the increase in confining stress due to the geocell.

The equivalent cohesion obtained for specimens reinforced with geocell GC150 was more pronounced than that obtained with geocell GC075. GC150 enclosed the entire cross-section of the specimen and, therefore, the increases in confining stress were greater. In the opposite

direction to that described for geocell GC075, this effect seems to decrease as the confining stress increases. These results are in accordance with expectations because the effect of geocells is more significant in poorly or moderately confined materials. The results demonstrated that these geocells may be a viable option for reinforcement in applications where soil confinement is relatively low, as is the case of unpaved roads. However, in situations where soil confinement is high, geocells may not be as effective or may even prove detrimental.

Table 1. Strength parameters for the soil and soil reinforced with the geocells G075 e G150.

Parameter	σ_3 (kPa)	Soil	Soil with GC075	Soil with GC150
Friction angle, ϕ (º)	-	40.5	41.4	43.0
Increase in confining stress, $\Delta\sigma_3$ (kPa)	12	-	0.31	6.17
	25	-	2.31	7.40
	50	-	3.05	1.88
Equivalent cohesion, c_R (kPa)	12	-	0.34	6.69
	25	-	2.51	8.03
	50	-	3.31	2.05

The increase in confining stress and equivalent cohesion obtained were lower than those observed in other studies (e.g., [1, 2]). Several possible explanations for these results are hypothesised next. On the one hand, the tensile strength and stiffness of the geocells prototyped (which are not quantified in this study) may be lower than in other studies. These properties have a significant effect on the ability of the geocell to confine the soil (stiffer geocells provide higher confinement and vice versa). In the same way, the geocells could only confine a small portion of soil in the middle of the specimens so their confining effect was limited to this region. The soil beyond the influence of the geocells tended to behave like the unreinforced material. On the other hand, the ratio between the opening of the geocell pocket and the soil particles size must also play a key role. As mentioned, $D_{max,c}/d$ and $D_{50,c}/d$ are ~10 times larger than the values reported in literature (mainly because of the type of soil considered, SW-SM). Geocells with high ratios can hinder the installation process, which in turn can have a significant impact on their performance. These ratios must be low enough to ensure that: i) the particles' arrangement within the soil skeleton is adequate; ii) no voids form in the vicinity of the geocell; iii) the location and geometry of the geocell within the soil is not altered during installation; iv) and the geocell is not an obstacle to water drainage or does not create preferential paths for water percolation. The results suggest that the laboratory studies presented in the literature, mainly using geocells with small openings and sands, may not be representative of the behaviour of the majority of commercially available geocells (with larger pocket openings) and of infill materials used in unpaved roads.

Finally, it should be noted that the results obtained for geocell GC075 must be read with caution and considering the limitations mentioned below. The results obtained with this geocell are affected by the fact that the test specimen is considerably larger than the opening of the geocell pocket. In practice, geocells are made up of several adjacent and connected pockets. This study aims to compare the effect of a single pocket geocell on the behaviour of the soil. The results show that this geocell is not efficient because it does not confine the entire cross-section of the specimen. To show its true potential, the tests needed to be carried out on a smaller specimen (with diameter equal to the aperture of the geocell). However, in such case, additional particles would have to be removed from the soil.

4 Conclusions

This study aimed to investigate the stress-strain response of a locally sourced soil reinforced with 3D printed single pocket geocells, under triaxial conditions. An experimental program was conducted, including the characterization of soil properties, the design and fabrication of single pocket geocells using 3D printing, and triaxial testing of unreinforced and reinforced soil specimens.

The study showed that the inclusion of 3D printed single pocket geocells enhanced the mechanical properties of the soil. These geocells increased the soil's peak friction angle, which can be compared to an additional confining stress, i.e., improved stress-strain performance. While both reinforcement configurations evaluated improved soil strength, geocell GC150 showed significantly greater effects, particularly under low confining stress conditions (such as those in unpaved roads). However, it must be noted that the results suggest limitations in using geocells under high-confinement scenarios due to reduced incremental benefits.

The practical implementation of 3D printing technology could optimize material usage and improve the sustainability of forest road construction. Further research is recommended to explore the durability and field performance of geocells in diverse soil and environmental conditions (including, large-scale laboratory and field tests with multiple pocket geocells). By integrating sustainability principles with advanced material technologies, this research contributes to the development of more durable, cost-effective, and environmentally friendly solutions for unpaved forest road construction.

Acknowledgements and Fundings: This study was funded by the PRR—Recovery and Resilience Plan and by the NextGenerationEU funds at Universidade de Aveiro, through the scope of the Agenda for Business Innovation "Transform - Transformação digital do setor florestal para uma economia resiliente e hipocarbónica" (Project no.34 with the application C644865735-00000007). This work was also supported by FCT – Fundação para a Ciência e Tecnologia, I.P. by project reference UIDB/04625/2025 of the research unit CERIS.

Data availability statement: Data are contained within the article.

Author contribution statement: Conceptualization, D.M.C., J.M., M.P.-L.; methodology, D.M.C., J.M., M.P.-L.; validation, D.M.C., J.M., M.P.-L.; formal analysis, D.M.C., J.M., M.P.-L.; investigation, D.M.C.; resources, O.C., J.M., M.P.-L.; data curation, D.M.C., J.M., M.P.-L.; writing - original draft preparation, D.M.C., M.P.-L.; writing - review and editing, D.M.C., O.C., J.M., M.P.-L.; visualization, D.M.C., J.M., M.P.-L.; supervision, J.M., M.P.-L.; project administration, J.M., M.P.-L.; funding acquisition, O.C., J.M., M.P.-L. All authors have read and agreed to the published version of the manuscript.

References

1. R.H. Chen, Y.W. Huang, F.C. Huang, Confinement effect of geocells on sand samples under triaxial compression. Geotext. Geomembr., **37** (2013). https://doi.org/10.1016/j.geotexmem.2013.01.004
2. R.J. Bathurst, R. Karpurapu, Large-Scale Triaxial Compression Testing of Geocell-Reinforced Granular Soils. Geotech. Test. J., **16**, 13 (1993).
3. X. Sun, X. Tang, W. Zhang, Magnified resilient behavior of recycled aggregates due to lateral restraint of geosynthetic under cyclic loading. Transp. Geotech., **45**, 101206 (2024). https://doi.org/10.1016/j.trgeo.2024.101206

4. A. Krishna, G.M. Latha, Fabrication and Testing of Low Strength Geocells Using 3D Printed Polypropylene Sheets. Int. J. Geosynth. Ground Eng. **10** (2024). https://doi.org/10.1007/s40891-024-00547-1
5. H. Lei, T. Ma, S. Feng, L. Wang, Confinement effect of geocell on the mechanical characteristics of reinforced sand subgrade. Transp. Geotech., **48**, 101336 (2024). https://doi.org/10.1016/j.trgeo.2024.101336
6. I. Amurane, M. Zhang, T. Li, H. Jiang, Optimization of 3D printed geocells based on numerical simulation and experimental investigation. Earth Environ. Sci., **233,** 032043 (2019) https://doi.org/10.1088/1755-1315/233/3/032043
7. American Society for Testing and Materials (ASTM) (2011). D 2487-11 Standard Practice for Classification of Soils for Engineering Purposes (Unified Soil Classification System)
8. European Committee for Standardization (CEN) (2012). EN ISO 933-1:2012 Tests for geometrical properties of aggregates — Part 1: Determination of particle size distribution — Sieving method
9. International Organization for Standardization (ISO) (2004). ISO/TS 17892-12:2004 Geotechnical investigation and testing — Laboratory testing of soil — Part 12: Determination of Atterberg Limits
10. American Society for Testing and Materials (ASTM) (2007). D1557-07 Standard Test Methods for Laboratory Compaction Characteristics of Soil Using Modified Effort (56,000 ft-lbf/ft^3 (2,700 kN-m/m^3))
11. International Organization for Standardization (ISO) (2004). ISO/TS 17892-3:2004 Geotechnical investigation and testing — Laboratory testing of soil — Part 3: Determination of particle density
12. International Organization for Standardization (ISO) (2004). ISO/TS 17892-9:2004 Geotechnical investigation and testing — Laboratory testing of soil — Part 9: Consolidated triaxial compression tests on water-saturated soils
13. D.J. Henkel, G.C. Gilbert, The Effect of Rubber Membranes on the Measured Triaxial Compression Strength of Clay Samples. Geotechnique, **3**, 1 (1952)
14. M. Budhu, Soil mechanics and foundations (John Wiley and Sons, New York, 2010)